PHYSICAL REVIEW B

CONDENSED MATTER

THIRD SERIES, VOLUME 29, NUMBER 2 15 JANUARY 1984

Energy distributions of pulsed-laser field-desorbed gaseous ions and field-evaporated metal ions: A direct time-of-flight measurement

T. T. Tsong and T. J. Kinkus

Physics Department, The Pennsylvania State University, University Park, Pennsylvania 16802

(Received 6 September 1983)

Energy distributions of pulsed-laser field-desorbed gaseous ions and field-evaporated metal ions have been obtained by directly measuring their flight times in the pulsed-laser atom-probe field-ion microscope. Energy distributions of gaseous ions show the same critical energy deficit, $I-\phi$, and the same general characteristics, namely a sharp rise at the high-energy side and a slowly decaying tail with resonant secondary peaks at the low-energy side, as those found in field ionization. However, the width of the main peak does not widen with increasing field as in field ionization. Energy distributions of field-evaporated metal ions, in general, are more symmetrically shaped with no prominent low-energy tails. A small low-energy tail can be seen for highly charged ions if the field-evaporated ions consist of another lower-charge-ion species of nearly equal abundance. The critical-energy deficit of these ions is consistent with the expression $\Lambda+\sum_i I_i-n\phi-Q$. No surface-plasmon excitations are evident in field ion emission. The energy distribution of pulsed-laser field-desorbed H_3^+ ions resembles more closely those of field-evaporated metal ions. Based on these observations, mechanisms of pulsed-laser field desorption and field evaporation of different types of ions have been proposed.

I. INTRODUCTION

Field desorption (field evaporation) is a phenomenon where surface atoms, either adsorbed atoms or substrate atoms, can be removed from the surface by an applied high electric field at low temperatures.[1,2] Being a relatively simple desorption phenomenon, it is of considerable theoretical interest. It is also of considerable practical interest. In atom-probe and field-ion microscopy, field evaporation is used to produce an atomically smooth and clean surface, to reach the bulk of a sample, and to facilitate atomic-layer—by—atomic-layer compositional analysis of a sample by the time-of-flight mass spectrometry, etc. Field evaporation is also one of the steps involved in the ion formation in a liquid-metal ion source. It is a high-brightness ion source with many applications.[3]

Direct information for understanding the mechanisms of field desorption is found in the energy distribution of the ions.[4] When there is no internal energy change of the desorbing species, the energy distribution reflects directly the spatial regions where the ions are formed. For example, in field ionization the existence of a critical distance and the narrowness of the ionization disk, or zone, have been deduced from the sharp onset energy and the narrow width observed in the field-ion-energy distribution.[5]

High-resolution energy distributions of field-desorbed gas ions and field-evaporated metal ions from atomically well-defined surfaces are more difficult to obtain than those in field ionization. The difficulties are the following. (a) In field evaporation only a very small number of ions can be collected before the field at the emitter surface is changed significantly by the increasing radius of the emitter. (b) In field desorption of adsorbed gas species we know that field-adsorbed inert-gas atoms cannot be desorbed without also field-evaporating the substrate atoms.[6] Although some chemisorbed species can be desorbed prior to the field evaporation of the substrate, the desorption field is usually so high that field dissociation of the desorption species almost always occurs. (c) Field desorption by high-voltage pulses introduces a large energy spread of the ions which is not intrinsic to the desorption process itself.[7] Because of these difficulties, few energy distributions of field-desorbed gaseous ions have been measured. The few energy distributions taken for metal ions are all obtained by heating the emitter to several hundred degrees Kelvin to sustain a nearly constant ion current.[8] The surface condition is poorly defined since a field- and temperature-induced dissociation of surface planes can occur. The field evaporation may also be affected by impurity atoms which may diffuse to the tip apex from the shank at high temperatures. The energy resolution is also limited.

These difficulties can be overcome by using the pulsed-laser atom probe that has been briefly described recently[9] and will be further discussed in the following sections. We will show that the basic mechanism of laser-induced desorption is thermally assisted field desorption; the heating is done very quickly, so that time-of-flight measurements can be performed with high resolution. We present here a detailed study of the energy distribution of pulsed-laser field-desorbed gaseous ions, field-evaporated metal ions, and field-evaporated metal-gas complex ions in metal helide and hydride formation. From the data obtained, we will suggest mechanisms of ion formation in these cases, and will try to shed some light on a few outstanding questions, such as surface-plasmon excitation and post field ionization in the field-evaporation process.

II. EXPERIMENTAL METHOD

The instrument used in this study is the newly developed[10] linear-type pulsed-laser time-of-flight atom-probe field-ion microscope shown in Fig. 1. It uses laser pulses of $\lambda=337$ nm and width 300 ps from a Nitromite laser model 103 by the Photochemical Research Company for the fast-pulse field desorption needed in a time-of-flight mass and energy analysis. The flight path is ~ 425 cm, and the probe-hole diameter is ~ 3 mm which has an angular extension of $\sim 1°$ to the tip.

Before a field-desorption experiment, the emitter surface is always developed to atomic perfection by low-temperature field evaporation in helium or neon. After aiming the probe hole of the atom probe to a desired area of the surface, by adjusting the gimbal system, the image gas is pumped out until the vacuum reaches low, 10^{9} Torr or lower, pressure, before a desired gas for the field-desorption study is introduced into the system. The gas pressure is usually kept in the 10^{-8}-Torr range so that the signals detected come only from the adsorbed state. Laser pulses heat the tip surface, typically 200—300 K, as estimated from the evaporation field of the substrate. The field-desorbed ions are collected one by one from a circular area covered by the probe hole which is 2—8 atomic diameters in size depending on the radius of the emitter used. Signals are recorded on oscilloscope (Tektroniks model 485-2) traces as shown in Fig. 2. In a time-expanded mode at 50 ns/div, the flight-time difference of the ions can be measured to an accuracy of $\sim\pm 1.25$ ns, which is better by a factor of 4 than the 200-MHz electronic timer we now have.

The kinetic energy of an ion can be determined if its mass and speed are known accurately. While the masses of elements are known to an accuracy of at least eight significant figures, the accuracy of a time measurement with an oscilloscope is very poor. Fortunately the oscilloscope can measure the flight-time difference of two ions of nearly identical masses and energies with an accuracy of $\sim\pm 1.25$ ns. Therefore the energy of an ion can be determined accurately by comparing its flight time with that of an ion of known energy and comparable mass.[9] This method will be obvious when we discuss the critical-energy-deficit measurement.

The flight time and the energy of an ion are related to each other by

$$E=\tfrac{1}{2}Mv^2=\tfrac{1}{2}M\frac{l^2}{t^2}=neV-\epsilon\,, \tag{1}$$

where M is the ion mass, v is the speed, l is the flight-path

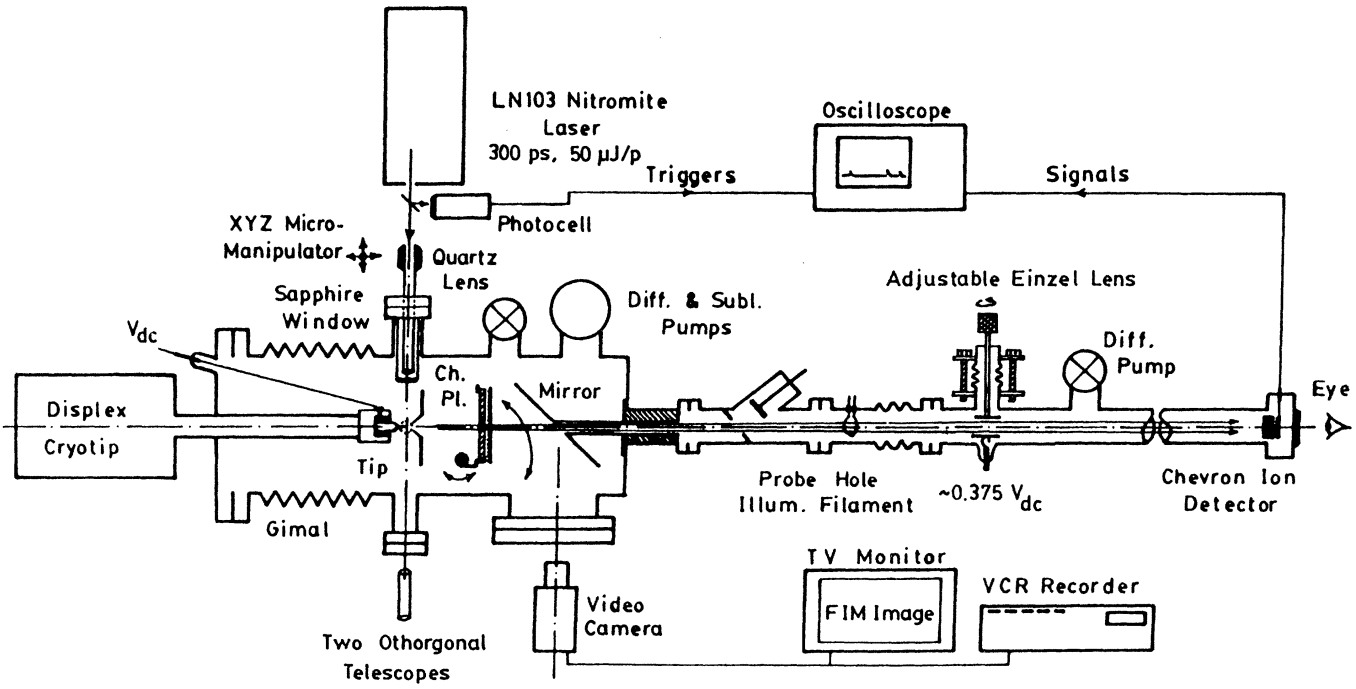

FIG. 1. Schematic diagram of the pulsed-laser time-of-flight atom-probe field-ion microscope used in this study. It is a high-resolution mass spectrometer and ion-energy analyzer of single-ion detection sensitivity. Ions are collected from a small area of the emitter surface, covering a few to about 20 atoms.

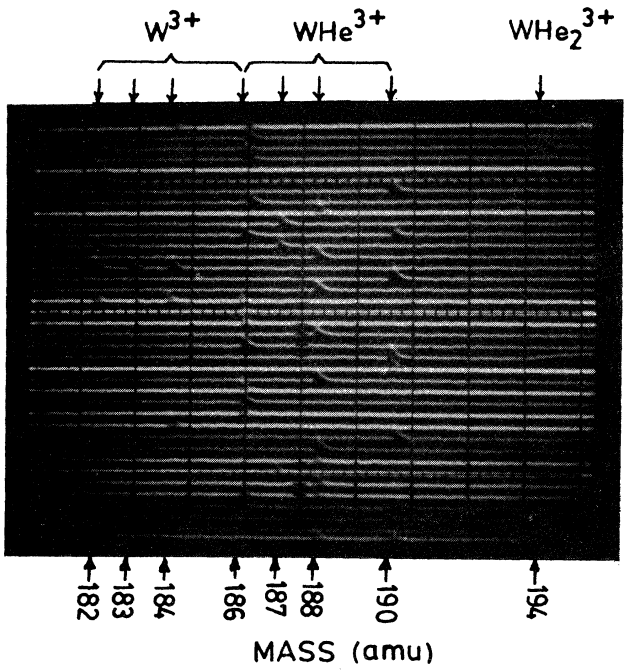

FIG. 2. Oscilloscope with 38 traces, at 0.1-μs/div speed, showing the time-of-flight signals in a study of tungsten-helide formation. Ions are detected one by one. Because of the exceptional mass resolution of this atom probe, no ambiguity exists in properly identifying the ion species even if some of them are rare.

length, t is the flight time, V is the accelerating voltage, n is the charge state, and ϵ is the energy deficit of the ion. As the energy spread of field-desorbed ions is usually less than 0.5% of the total ion energy, the energy spread and time spread are related to each other by

$$\Delta E \cong -\frac{[2(neV-\epsilon)]^{3/2}}{lM^{1/2}}\Delta t \cong -C\,\Delta t\ , \tag{2}$$

where C is a proportionality constant. The approximation signs come from the fact that ϵ is not really a constant, but has a very small variation. Thus the energy and flight-time distributions of the ions are linearly proportional to each other as long as the energy spread is small compared to the total ion energy. It can also be shown that[6]

$$\frac{\delta E}{E} = -\frac{2\,\delta t}{t} + \frac{\delta M}{M} + \frac{2\,\delta l}{l}\ . \tag{3}$$

The mass resolution of the pulsed-laser atom-probe had been discussed in some detail earlier.[10] We consider here the energy resolution of the system in the ion-energy analysis. For a given ion species, $\delta M = 0$. The energy resolution of the system is limited by Δl and δt, the maximum flight-path variation of the ions and the uncertainty in the flight-time measurement. For the given geometrical configuration of our system, under a proper ion-focusing scheme, $2\,\delta l/l \approx 3\times 10^{-5}$. This is a constant factor which does not depend on the experimental conditions of the measurement. δt comes from at least three sources, the resolution of the time-measuring device, the laser-pulse width, and the cooling time of the tip once it is heated by a laser pulse. The laser-pulse width, 300 ps, is negligibly short. The uncertainty in the flight-time measurement, using the method just described, is about 1.25 ns. The cooling time of the tip depends on the tip material, the tip shape, the initial tip temperature, and the incident laser power and duration. Our calculation[11] indicates that if the incident power of the laser and the tip-temperature rise are low (therefore the thermal conductivity is high), then within ~ 1 ns, the tip temperature can decrease by 10 K, sufficient to reduce the desorption rate significantly. For our estimation here, $\delta t \approx 2$ ns or less. The total flight time of an ion varies with the mass, the charge state, and the emitter voltage. Under typically good operating conditions for the ion-energy analysis, the flight time ranges from ~ 5 μs for light ions such as H^+ to ~ 60 μs for heavy ions such as Au^+. Values of $2\delta t/t$ therefore range from $\sim 8\times 10^{-4}$ to $\sim 7\times 10^{-5}$. The energy resolution, defined as

$$\delta E/E = [(2\delta t/t)^2 + (2\delta l/l)^2]^{1/2}\ ,$$

varies from 8×10^{-4} to 8×10^{-5}. To achieve high energy resolution in the energy analysis, one must choose ions of a large mass and field desorb them at a very low tip voltage. These conditions, of course, cannot be always satisfied, and compromises often have to be made.

The typical tip voltage used in our experiment ranges from 2 to 4 kV for gas ions. For studying field evaporation, the number of ions which can be collected before the field is significantly changed is very small for small-radius tips. Compromises have to be made, and we generally use tip voltages around 4—8 kV. In Fig. 3 an energy distribution of pulsed-laser field-desorbed N_2^+ ion from the W(110) lattice steps and terraces taken at $V_{dc} = 2000.0 \pm 0.1$ V is shown (curve *B*). The full width at half maximum (FWHM) is only ~ 2.1 eV, which corresponds to ~ 19.4 ns in the flight-time distribution. The onset energy, or the critical-energy deficit of the ions, can be determined to an accuracy of ± 0.1 eV; this corresponds to $\delta t = \pm 2$ ns. This capability is demonstrated with the help of another ion-energy distribution taken at 2002.0 ± 0.1 V (curve *A*). Although the number of ions collected is small and statistical fluctuations large for this distribution, it has the same FWHM of ~ 2.1 eV. The onsets of the two distributions, indicated by arrows *a* and *b*, correspond exactly to an energy difference of 2.0 eV. This figure demonstrates that high-resolution energy distributions of pulsed-laser-desorbed ions can be obtained if proper operating conditions can be met, and, in principle, the critical-energy deficit of field-desorbed ions can be determined to an accuracy of ± 0.1 eV. However, the ideal conditions are often difficult to satisfy, and some of the data to be presented here have not achieved this energy resolution.

III. PULSED-LASER FIELD DESORPTION OF GASEOUS IONS

The spatial origins of ions in field ionization and field desorption can be derived directly from the energy distri-

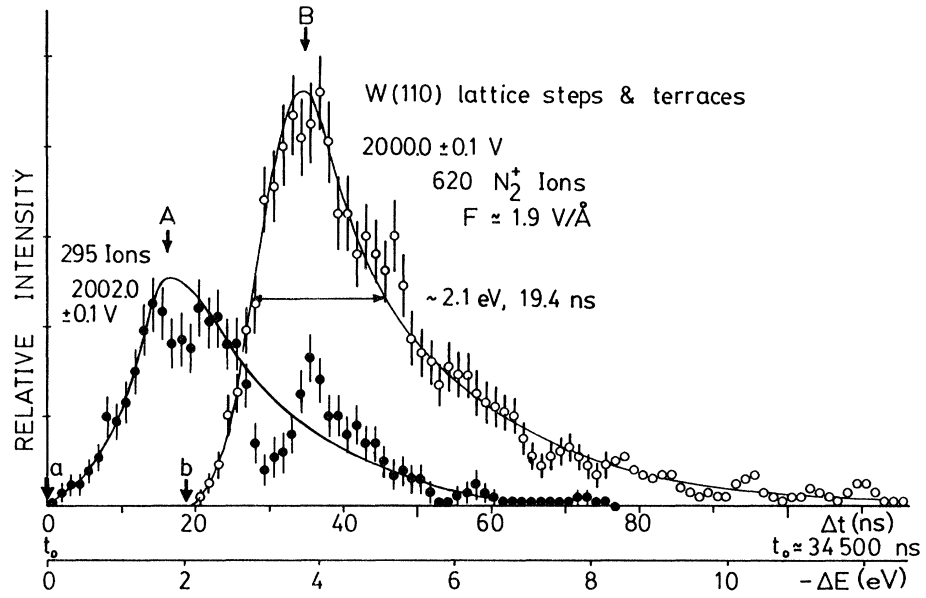

FIG. 3. Energy distributions of pulsed-laser field-desorbed N_2^+ ions taken at 2000.0 and 2002.0 V. Under this low voltage the leading edges of these distributions can be determined with an accuracy of ±0.1 eV.

butions of these ions. An ion of charge *ne*, originating at the surface, will acquire the full energy *neV* of the accelerating voltage *V*. On the other hand, if the ion is formed at a distance *x* from the surface, the ion will have an energy deficit of

$$\epsilon = ne\int_0^x F(x')dx' , \tag{4}$$

where $F(x')$ is the electric field at x'. Inghram and Gomer first reported a measurement of the energy distribution of hydrogen ions in field ionization using a magnetic-sector mass spectrometer.[4] From the observed narrow distribution width at low field and increasing width at high field, they conclude that the ions are formed near the surface at low field, and are formed further away from the surface by autoionization at high field. Muller and Bahadur,[12] and Tsong and Muller[5] measured energy distributions of inert-gas ions in field ionization using a retarding potential-energy analyzer. The latter authors showed that the FWHM of the distribution is only ~1 eV at low fields, thus establishing the ionization-disk thickness to be only ~0.2 Å. The width increases rapidly as the field is increased. They also confirmed the existence of a critical distance of field ionization, and found the measured critical-energy deficits of field ions to agree with the expression

$$\epsilon_c = I - \phi \tag{5}$$

given by Inghram and Gomer to within 0.5 eV. Since then many other studies have been reported. We report here a measurement of the energy distribution of pulsed-laser field-desorbed gaseous ions by directly measuring their flight times.

As already explained in Sec. II, it is easier to achieve high energy resolution by using heavier ions. In Fig. 4 an energy distribution of pulsed-laser field-desorbed Ne^+ ions collected from the W(110) lattice steps at ~4.5 V/Å is shown. A few interesting features are the following. (1) The general shape of the distribution is identical to that found in field ionization, i.e., a rapid rise on the high-energy side and a slowly decaying tail on the low-energy side. (2) The FWHM is about 2.6 eV, indicating that ions are formed within a spatial region of ~0.6 Å. (3) A secondary peak similar to those found by Jason *et al.* in field ionization[13] can be seen. Thus in every aspect, the pulsed-laser field-desorbed Ne ions resemble those Ne ions in field ionization.

Our method of flight-time measurement cannot achieve the nanosecond accuracy which is required to derive the

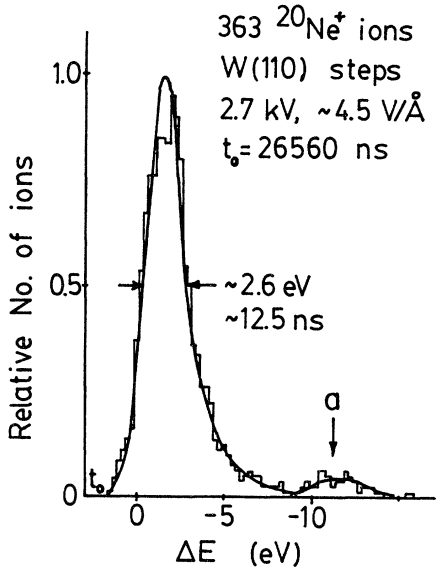

FIG. 4. Energy distribution of pulsed-laser field-desorbed Ne^+ ions taken at 2.700 kV and $F \approx 4.5$ V/Å from the W(110) lattice steps. First resonant tunneling peak (arrow a) is clearly visible even though the number of ions in the distribution is small.

critical-energy deficit of the ions. This difficulty is solved by comparing the flight times of two ion species of nearly identical masses as illustrated in Fig. 5. The ionic species of our choice are He^+ and $D_2{}^+$. The masses are, respectively, 4.0026 and 4.0282 amu; their mass difference is 0.0256 amu. If He^+ and $D_2{}^+$ ions had the same critical-energy deficit, then from the mass difference we would expect the leading edges of the He^+ and $D_2{}^+$ distributions to be separated by 31 ns as indicated by arrows *a* and *b*. In reality they are separated only by 20 ns (arrow *c*). Thus the most energetic $D_2{}^+$ ions have ~ 9 eV more energy than the most energetic He^+ ions. This data can be easily explained in terms of Eq. (5) if one realizes that the ionization energy of He, 24.6 eV, is 9.0 eV larger than that of D_2, 15.6 eV. Thus the pulsed-laser field-desorbed gas ions exhibit the same critical-energy deficit as in field ionization, and Eq. (5) is again confirmed to within the accuracy of our data which is about ± 0.5 eV.

The question now is whether or not there is any difference between pulsed-laser field desorption and field ionization, and if so whether it will show up in the energy distributions. This question is answered in Fig. 6, which shows the energy distributions of pulsed-laser field-desorbed Ar^+ ions at 2.2, 2.4, and 2.7 V/Å. The FWHM of the main peak of the three distributions remains unchanged when the field is raised from 2.2 to 2.7 V/Å even though the secondary peaks are slightly more pronounced at higher fields. In fact the FWHM of the flight-time distribution reduces from 27 to 20 ns as the field is raised from 2.2 to 2.7 V/Å. This behavior is in sharp contrast to field ionization where the FWHM increases rapidly as the applied field is raised above the best image field, ~ 2.2 V/Å for Ar. This observation indicates that in pulsed-laser field-desorption, autoionization is negligibly small because of very low gas pressure in the system, and ions are formed exclusively from the desorbed surface species.

Based on the above observations we can now formulate with some certainty a mechanism of pulsed-laser field desorption of gases which is illustrated in Fig. 7. Pulsed-laser field desorption is field ionization above the critical distance of gas molecules or atoms thermally desorbed from their adsorption states. The fact that few ions have energies larger than that limited by the critical-energy deficit indicates that a photoexcitation process is negligibly small on metal surfaces. Laser pulses heat the emitter surface for a brief period to cause the adsorbed species to desorb. When they pass through the ionization zone, a fraction of them are field-ionized. Thus the characteristics of the energy distribution of pulsed-laser field-desorbed gas ions closely resemble those in ordinary field ionization. The differences, i.e., the field independence and the nearly constant FWHM of the main peak, all result from the different ways of supplying the gas mole-

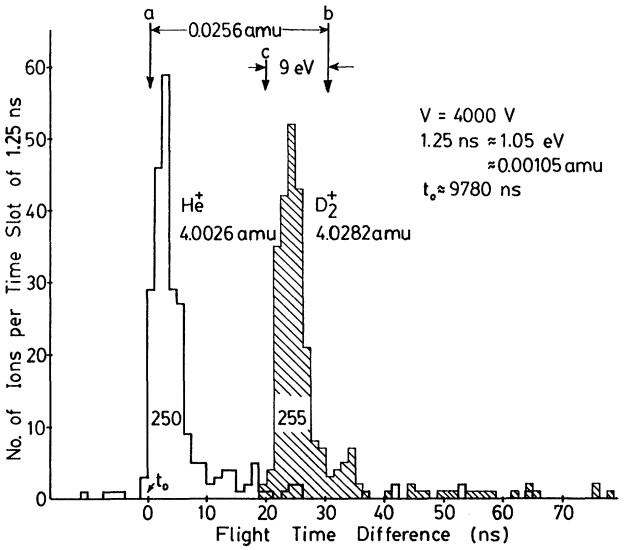

FIG. 5. Energy distributions of pulsed-laser field desorbed $^4He^+$ and $D_2{}^+$ ions. Although their masses differ only by 0.0256 amu, their mass lines are separated at $\sim 5\%$ of the peak height. Their leading edges are consistent with $\epsilon_c \approx I - \phi$, similar to those found in field ionization.

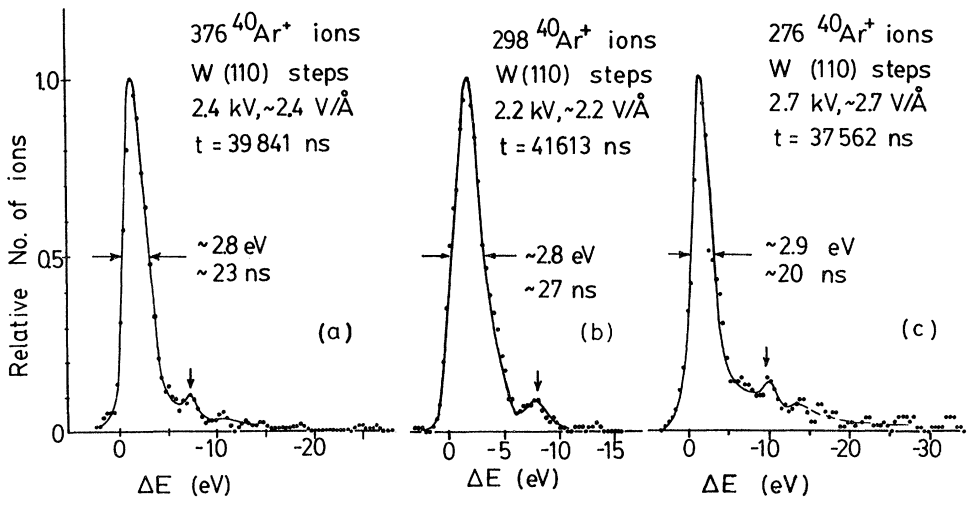

FIG. 6. Field dependence of the energy distribution of pulsed-laser field-desorbed ions. FWHM of the main peak remains nearly constant when the field is changed from 2.2 to 2.7 V/Å. Low-energy tail is more pronounced at 2.7 than at 2.2 V/Å.

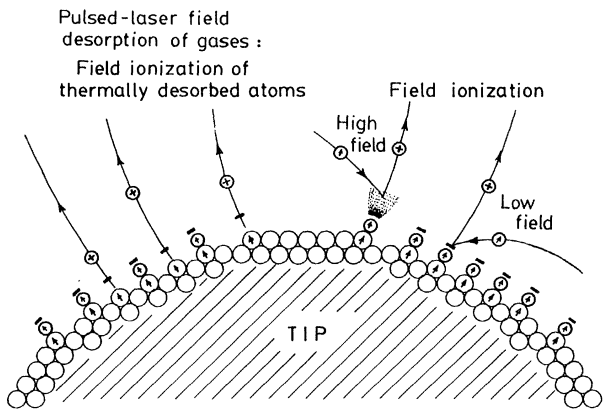

FIG. 7. Schematic diagram showing differences between field ionization and pulsed-laser field desorption of gases. Latter process is field ionization of flash-desorbed (thermal desorption in ps) surface species.

cules. In field ionization, many gas molecules hop around the emitter surface. Autoionization can occur at high fields. The energy distribution reflects the combined effect of the spatial variation of the electron-tunneling probability and the gas-density function. In pulsed-laser field desorption at low gas pressure, all of the pulsed, thermally desorbed adsorption species pass across the ionization zone only once. No gas-density function enters into the picture. At low field only a small fraction of the thermally desorbed molecules are field-ionized. This fraction increases as the field is raised. Thus the low-energy tail of the ion-energy distribution becomes more pronounced at higher fields. The energy distribution at the low-field limit, when the probability of field ionization in one passage is small, directly reflects the spatial variation of the tunneling probability of the atomic electron into the metal.

The clarification of the mechanisms of pulsed-laser field desorption of gaseous species has some practical significance. From the heating temperature of the laser pulses, which can be calibrated by observing the reduction of the evaporation field of the substrate,[14] one can tell whether the desorbed species comes from the chemisorbed, physisorbed, or field-adsorbed state, as in the ordinary flash-desorption technique. Since thermal desorption is one of the most gentle desorption processes (when compared to electron- or ion-impact desorption), and field ionization is also one of the most "gentle" ionization processes (when compared to particle-impact ionization processes), one can expect the desorption species observed at the low-field limit to reflect the true adsorption states of the species well.

IV. PULSED-LASER FIELD EVAPORATION OF METAL IONS

In field ionization, high-resolution ion-energy distributions can be obtained with a retarding potential-energy analyzer. In field evaporation the number of ions which can be collected without blunting the tip radius by more than a few percent is very small. High energy resolution cannot be achieved with the retarding potential-energy analyzer. In the pulsed-laser time-of-flight atom-probe, a high-resolution ion-energy distribution can be obtained from a few hundred ions; they can be collected from a specific plane of the emitter surface without blunting the emitter radius more than 2—3 %.

In this study, we attempt to answer three questions. (1) What is the critical-energy deficit of field-evaporated ions, especially the multiply charged ions? (2) Do substantial surface-plasmon excitations occur in field evaporation? (3) How are the multiply charged ions formed in field evaporation? Are they formed by stepwise post-field-ionization of singly charged field-evaporated ions, or by formation of a multiply charged ion in one step?

A. Critical-energy deficit in field evaporation

This problem has been investigated earlier by Tsong, Schmidt, and Franck.[15] By adapting the charge-exchange model of field desorption for electronegative gases proposed by Gomer,[1,16] to field evaporation of metals, they derive the critical-energy deficit of field evaporating as $n+$ ions to be

$$\epsilon_c(n)=\Lambda+\sum_{i=1}^{n} I_i-n\phi-Q_n\ , \tag{6}$$

where Λ is the sublimation energy, I_i is the ith ionization energy, ϕ is the work function of the surface, and Q_n is the activation energy for field evaporation. They have also presented data for singly charged silver ions measured with a retarding potential method, which are in excellent agreement with the expression. We want to show here that the expression is also valid for doubly charged ions, and therefore should be valid for multiply charged ions.

For this purpose we select $^{56}Fe^{2+}$ (27.9675 u) and N_2^+ (28.00615 u) as the ion species. Their mass-to-charge ratios differ by 0.03865 u. The pulsed-laser field-desorbed gas ions N_2^+ can be used as our reference since the critical-energy deficit of N_2^+ ions coming from an iron surface, $I-\phi=15.8-4.4$ eV$=11.4$ eV, is known. The experimental data are shown in Fig. 8. Arrow 1 indicates the leading edge of the N_2^+ energy distribution which is our reference. Arrow 2 indicates where the leading edge of N_2^+ ions should be if their energy were larger by 20 eV, in complete agreement with the other N_2^+ distribution taken at 20 V higher dc voltage. Arrow 3 shows where the leading edge of the $^{56}Fe^{2+}$ distribution should be if they do not suffer from any energy deficit. Arrow 4 is where the leading edge of $^{56}Fe^{2+}$ distribution should be if they suffer a critical energy deficit of $\epsilon_c^{(2)}\cong\Lambda+I_1+I_2-2\phi=4.29+7.90+16.16-2\times4.40$ eV $=19.55$ eV. The leading edge of the $^{56}Fe^{2+}$ distribution agrees with this arrow within about ±1 eV. The leading edge of the $^{56}Fe^{2+}$ distribution is in fact slightly ahead of the arrow, signifying that we have omitted the activation-energy term from Eq. (6) here. The activation energy should be on the order of 0.5 eV which will make the agreement between the experimental data and the calculation even better. Unfortunately, even though our data are accurate enough to confirm the validity of Eq. (6), they are not yet accurate enough to determine the activation energy in field evaporation. Only when sub-

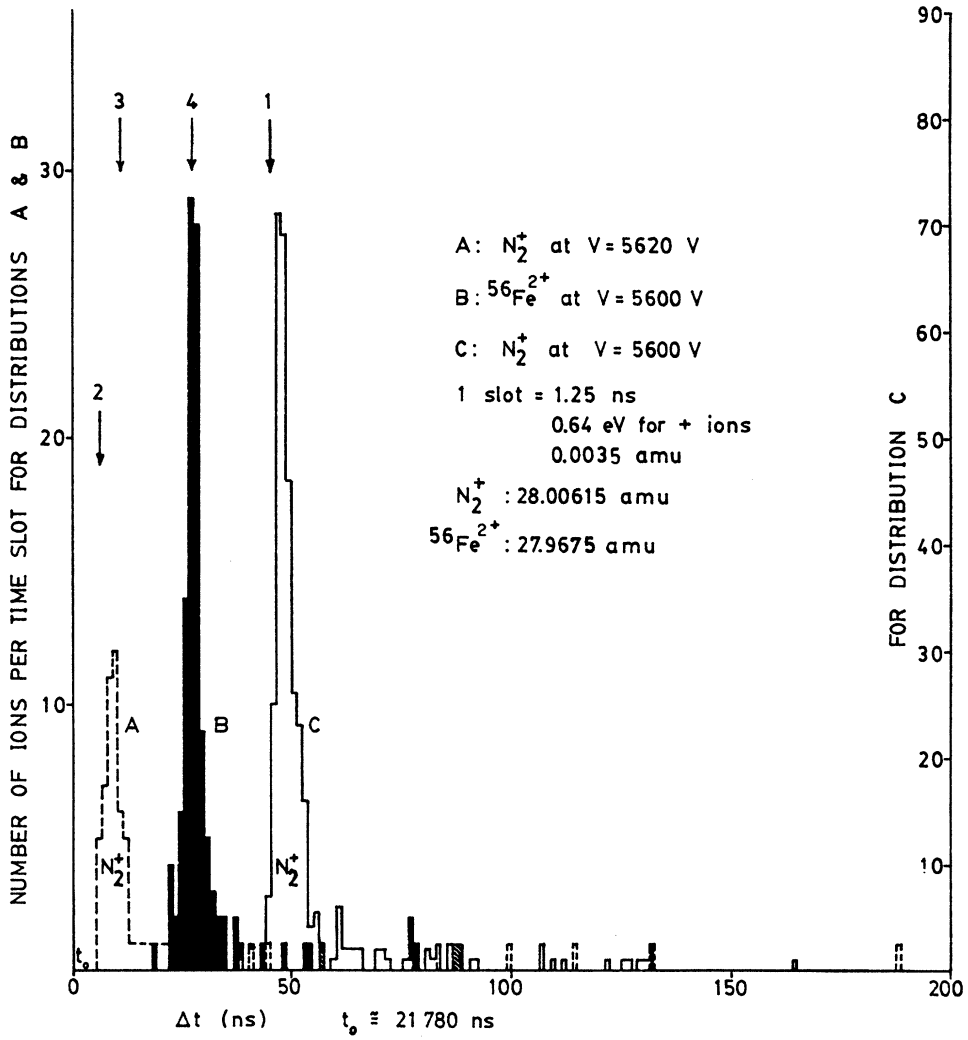

FIG. 8. Energy distributions of pulsed-laser field-desorbed N_2^+ and $^{56}Fe^{2+}$ ions. FWHM's are very narrow. From these distributions we conclude that $\epsilon_c \approx \Lambda + \sum_i I_i - n\phi - Q$ is valid for multiply charged field-evaporated metal ions.

nanosecond timers become available can the required energy resolution be achieved.

B. Surface-plasmon excitation in field evaporation and field ionization

In field ionization Jason *et al.* find an oscillatory tail in the energy distribution which they explain in terms of a resonance tunneling effect.[13] Lucas, on the other hand, explains that the structure arises from multiple surface-plasmon excitations caused by the ensuing ions.[17] If surface-plasmon excitations can occur from singly charged field ions formed about 4 Å away from the surface, then the multiply charged ions formed right above the surface in field evaporation should be able to excite surface plasmons even more effectively. In fact calculations predict that as many as 60—100 surface-plasmon quanta can be excited by a field-evaporating metal ion. Lucas and Sûnjic[18] claim that this excitation is responsible for the large ion-energy spread observed in the nanosecond high-voltage pulse-operated atom probes. Müller and Krishnaswamy, on the other hand, explain that the large ion-energy spread results from a premature field evaporation.[7]

This problem is of considerable interest. Besides the controversies which obviously should be resolved, we are particularly interested in the possibility of using field evaporation to probe the fundamentally interesting surface-plasmon—excitation process. We approach this problem in the following way. Since nanosecond high-voltage pulses may produce a large ion-energy spread in field evaporation, this effect has to be isolated from the study. The fast pulsed-field evaporation needed for the time-of-flight energy analysis can be accomplished by picosecond laser pulses which will induce a negligibly small ion-energy spread of $\sim kT$ by a heating effect. Such a small energy spread will not be confused with the surface-plasmon excitations.

We have collected a large number of the energy distribution of field-evaporated metal ions. Shown in Fig. 8 is an energy distribution of $^{56}Fe^{2+}$ ions. Aside from a few scattered ions, there is no prominent low-energy tail similar to those observed in gaseous ions. According to Lucas,

the probability of a surface-plasmon excitation is proportional to n^2, where n is the charge state of the field-evaporating ion. The effect of surface-plasmon excitations should be much more pronounced for highly charged ions. Figure 9 shows an energy distribution of W^{3+} ions and also of WHe^{3+} ions, obtained under the condition that only 3 + ions are present, and by combining ions of all the major isotopes according to their masses. Again no low-energy tail can be seen. We therefore conclude that no substantial surface-plasmon excitations occur in field evaporation. The theory of Lucas and Sunjic grossly overestimates the probability of surface-plasmon excitations in field ion emission. Since multiply charged metal ions originating very close to the surface do not induce any substantial surface-plasmon excitations, neither will singly charged gas ions formed ~4 Å above the surface. The low-energy tails observed in field ionization and in pulsed-laser field desorption of gaseous ions are most probably produced by a resonance tunneling effect.[13]

C. Post-field-ionization in field evaporation

Using the image hump model of field evaporation, Brandon,[19] arrives at the conclusion that most metals will field-evaporate as doubly charged ions at low temperatures. This calculation is performed by setting the activation energy of field evaporation as n^+ ions $Q_n(F_n)=0$ and finding the value of F_n, which he defines as the evaporation field. For most metals, F_2 has the lowest value. For a few metals F_3 has the lowest value, thus they will field-evaporate as triply charged ions. Tsong[20] finds the charge-exchange model to give a similar result if the atom-to-surface plane distance is taken to be the radius of the metal atoms. In general, low-temperature field-evaporation results agree well with these calculations.[21] In high-voltage-pulse atom-probe experiments many investigators find that the charge states in fact are field dependent; highly charged ions such as W^{6+} can be formed if the applied field is sufficiently high.[22] Although highly charged ions can also be expected from the same calculations if the field is sufficiently high,[21] an alternative explanation, the post-field-ionization of field-evaporated ions, has also been pursued.[23]

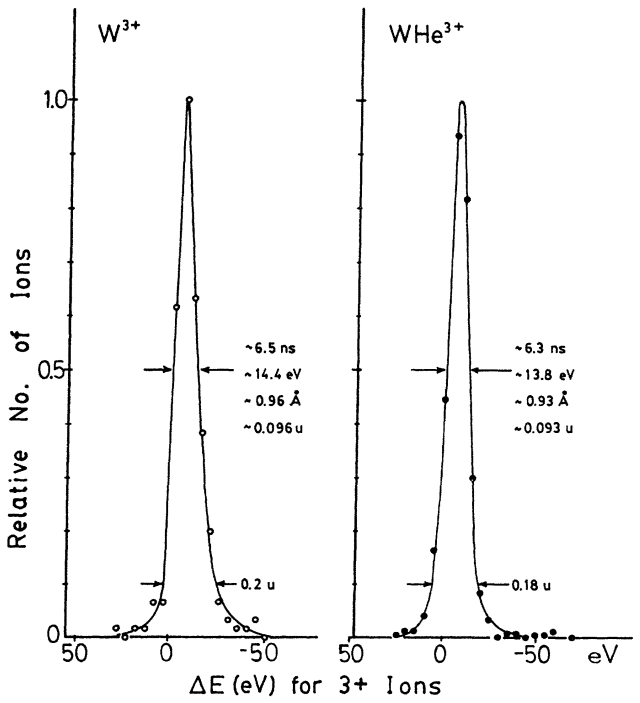

FIG. 9. Energy distributions of W^{3+} and WHe^{3+} ions taken under the condition that only the 3 + state is present. No low-energy tail can be seen. Also, both distributions have a comparable FWHM.

Chambers *et al.*[24] have made detailed calculations of the probability of post-field-ionization of field-evaporated ions and find it highly unlikely. Recently, new calculations by Kingham and Haydock, however, show quite convincingly that the observed multiply charged metal ions are all formed by post-field-ionization of singly charged field-evaporated ions.[23] Experimental results on the field dependence of the charge states of field-evaporated ions, obtained by Ernst and co-workers,[25] Kellogg,[26] and Konishi *et al.*,[27] seem to strongly support Kingham's calculations.[23]

All of the available experiment tests of the theory of post-field-ionization are based on the field dependence of the charge states of field-evaporated ions. In this type of measurement the applied field is a critical parameter, yet it changes continuously during an experimental measurement, and no accurate field calibration has been performed. We present here an alternative experiment to test the theory, i.e., by a measurement of the energy distribution of the multiply charged field-evaporated ions. In this type of experiment the applied field is not a critical parameter.

The first question we ask is how the critical-energy deficit of $n+$ ions formed by stepwise post-field-ionization differs from that of $n+$ ions formed by a simultaneous transition, or stripping, of n electrons from the atoms to the vacant metal states. The critical-energy deficit of the latter process has already been derived[15] and is given by Eq. (6). Let us consider here the simplest case in post-field-ionization: formation of doubly charged ions by post-field-ionization beyond the critical distance $x_c^{(2)}$ of the singly charged field-evaporated ions. When the singly charged ions are formed by field evaporation, the critical-energy deficit of the ions is given by

$$\epsilon_c^{(1)}=I_1+\Lambda-\phi-Q_1 , \tag{7}$$

where Q_1 is the activation energy of field evaporation. An additional critical-energy deficit is introduced when they are post field ionized beyond $x_c^{(2)}$. Hence,

$$\Delta\epsilon_c^{(2)}=eF_0x_c^{(2)}=I_2-\phi . \tag{8}$$

The total critical-energy deficit for forming 2 + ions by post-field-ionization is therefore given by

$$\epsilon_c^{(2)}=\epsilon_c^{(1)}+\Delta\epsilon_c^{(2)}=\Lambda+I_1+I_2-2\phi-Q_1 . \tag{9}$$

This expression is exactly the same as Eq. (6) except that Q_2 is now replaced by Q_1. In an experimental measure-

ment these two terms represent the same quantity, the activation energy of field evaporation. The difference in the notations arise purely from theoretical considerations. We can now conclude that the critical-energy deficit we measured for $^{56}Fe^{2+}$ agrees with both theories of field evaporation and cannot shed any light on which of the two theories is the valid one.

The second question concerns the low-energy tail observed in field ionization and in pulsed-laser field desorption of gaseous ions. If multiply charged metal ions are produced by stepwise field ionization of field-evaporated singly charged ions, one can expect these multiply charged ions to also show low-energy tails, especially for those highly charged ions such as W^{3+} where two post-field-ionization steps are involved. All of our energy distributions of multiply charged metal ions, taken under the condition that only one charge state is dominant, do not show any appreciable low-energy tail. One can argue that the ionization rate for post-field-ionization under such a condition is so large that all the low-charge-state ions are completely post-field-ionized within a narrow zone above the critical distance.

A better test is to observe the energy distribution of singly (or doubly) charged ions and doubly (or triply) charged ions taken under the condition that they are nearly equally abundant, so that half of the field-evaporated ions are not post-field-ionized. In Figs. 10 and 11 energy distributions of Ni^+ and Ni^{2+}, and Re^{2+} and Re^{3+} ions, taken under this condition are shown. Indeed, the Ni^{2+} and Re^{3+} ion-energy distributions show slightly wider FWHM's than those of Ni^+ and Re^{2+}. The former distributions also show noticeable low-energy tails, even if they are much less prominent that those in gas ions. For the Ni^+ and Re^{2+} distributions, aside from a few scattered ions, there are no low-energy tails. Our ion-energy distributions therefore also favor the post-field-ionization theory of forming multiply charged ions in field evaporation. We have to warn here that while the field dependence of ion-charge states has been calculated in great detail for the post-field-ionization model, no similar calculation exists for the single-step ion-formation model. Also, no calculation has been reported for the ion-energy distribution for either model. When such calculations become available, more meaningful comparisons with the experimental data can then be carried out.

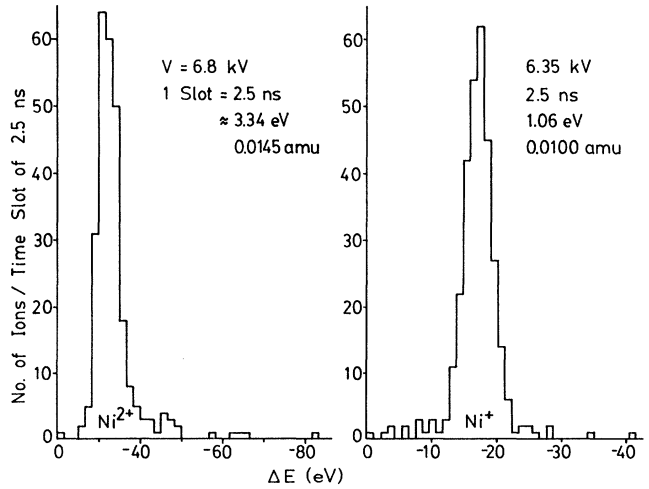

FIG. 10. Energy distributions of Ni^{2+} and Ni^+ ions taken under the condition that these two ion species are nearly equal in abundance.

D. Pulsed-laser field desorption of H_3^+ ions

In pulsed-laser field desorption of hydrogen,[9] many H_3^+ ions have been found in the field range 2.0—3.0 V/Å. A brief introduction to the subject and a detailed description of our pulsed-laser work have been presented recently[9] and will not be repeated here. Here we discuss, separately, H_3^+ formation from other gaseous ions for the following reasons. (1) H_3 is not stable in the gas phase even though H_3^+ has been known to be stable since its first observation[28] by J. J. Thomson in 1912. (2) As will be clear from further discussions, the energy distribution of pulsed-laser field-desorbed H_3^+ ions is distinctively different from all other pulsed-laser field-desorbed gaseous ions we have studied such as He^+, Ne^+, Ar^+, Xe^+, H_2^+, D_2^+, and N_2^+. The energy distributions of all these ions show substantial low-energy tails, and their critical-energy deficits are given by $I-\phi$.

To obtain the critical-energy deficit of the energy distribution of pulsed-laser field-desorbed H_3^+ ions, we again resort to another ion species of nearly identical mass, but with a known critical-energy deficit. The species of our choice is $^3He^+$. The masses of H_3 and ^3He are, respectively, 3.023 475 and 3.016 030 amu, and their mass difference

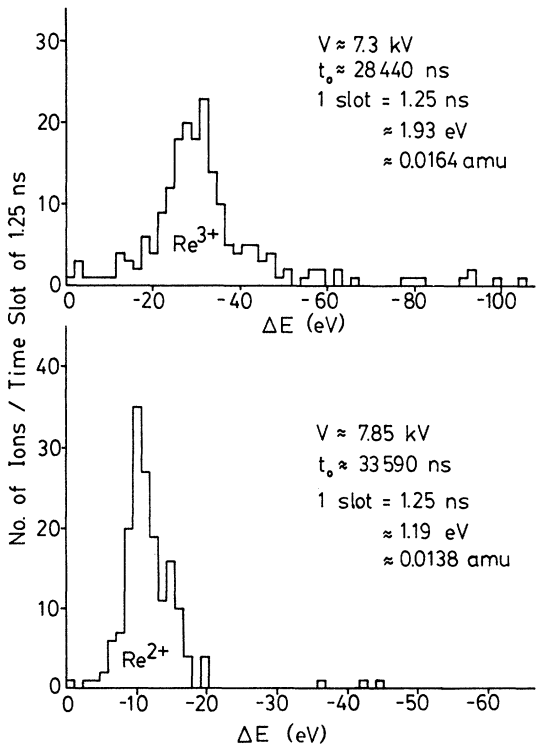

FIG. 11. Energy distributions of Re^{3+} and Re^{2+} ions taken under the condition that they are nearly equal in abundance.

is 0.00745 amu. Figure 12(a) shows a time-of-flight mass spectrum of H_3^+ and $^3He^+$ taken at 2400 V. Arrow *A* indicates where the leading edge of the $^3He^+$ distribution is located. If the H_3^+ ions had the same critical-energy deficit as the $^3He^+$ ions, then from the mass difference one would expect the leading edge of the H_3^+ distribution to be at the location indicated by arrow *B*. The experimental leading edge of the H_3^+ distribution is indicated by arrow *C*, which gives the critical-energy deficit of H_3^+ ions to be 12.5 eV less than that of ^3He ions. In other words, the most energetic H_3^+ ions have an energy larger than the most energetic $^3He^+$ ions by 12.5 eV, or

$$\epsilon_c(H_3^+)=\epsilon_c(^3He^+)-12.5\text{ eV}$$
$$\cong I_{He}-\phi_0-12.5\text{ eV}=12.1\text{ eV}-\phi_0\,, \qquad (10$$

where ϕ_0 is the work function of the clean Mo(110) steps where the $^3He^+$ and H_3^+ energy distribution are taken. That the H_3^+ ions are more energetic than the $^3He^+$ ions is shown in a very dramatic way in Fig. 12(b). In Fig. 12(a), at 2400 V, H_3^+ is about 15 ns ahead of $^3He^+$ even though its mass is 0.00745 amu larger. The H_3^+ and $^3He^+$ distributions are almost completely separated. At 3600 V, H_3^+ is only a few nanoseconds ahead of $^3He^+$ and the two distributions, or mass lines, overlap extensively. In fact at even higher voltages, $^3He^+$ will arrive slightly ahead of H_3^+ as it should from a consideration of only their masses; $^3He^+$ is the lighter species. The 3600-V data give an $\epsilon_c(H_3^+)\approx 12.6\text{ eV}-\phi_0$, in complete agreement with the 2400-V data. Our measurements thus give $\epsilon_c(H_3^+)\approx 12.4\text{ eV}-\phi_0$. The experimental uncertainty is $\sim\pm 0.5$ eV. In field ionization, $\epsilon_c+\phi_0$ is generally referred to as the appearance energy. The appearance energy of H_3^+, from field ionization of condensed hydrogen layers on W surfaces obtained by Jason *et al.*,[28] is 12.7 eV. Ernst and Block[29] report a measurement of the appearance energies of H_3^+ in field ionization, from W and Rh surfaces, to be, respectively, 12.3 and 11.4 eV. Except for the Rh data, for which they have recently changed their interpretations,[30] all of the H_3^+ appearance-energy data obtained from different metal surfaces by different investigators with slightly different physical processes, i.e., pulsed-laser field desorption and field ionization from condensed layers and ordinary field ionization, give a similar value of about 12.4 eV.

The question now is what the critical-energy deficit of H_3^+, or equivalently its appearance energy, really represents. If one uses the same expression used in field ionization, then

$$\epsilon_c(H_3^+)=I^*_{H_3}-\phi_H\,, \qquad (11)$$

where ϕ_H is the work function of the surface where H_3^+ data are taken; presumably, the surface is saturated with a chemisorbed layer of hydrogen. Our data, collected from the Mo(110) steps, then give

$$I^*_{H_3}\cong 12.4\text{ eV}+(\phi_H-\phi_0)\,. \qquad (12)$$

We have not been able to find, from the literature, $\phi_H-\phi_0$ for the Mo(110) steps at ~ 35 K. Polizzotti and Ehrlich[31] report $\phi_H-\phi_0=0.87$ eV for a field-evaporated W emitter surface saturated with hydrogen at 38 K. Since W and Mo surfaces are similar in electronic properties, $\phi_H-\phi_0$ for the Mo(110) steps should be a positive quantity with a value of about 0.8 eV. The appearance energy derived, $I^*_{H_3}=13.2$ eV, is much larger than the expected ionization

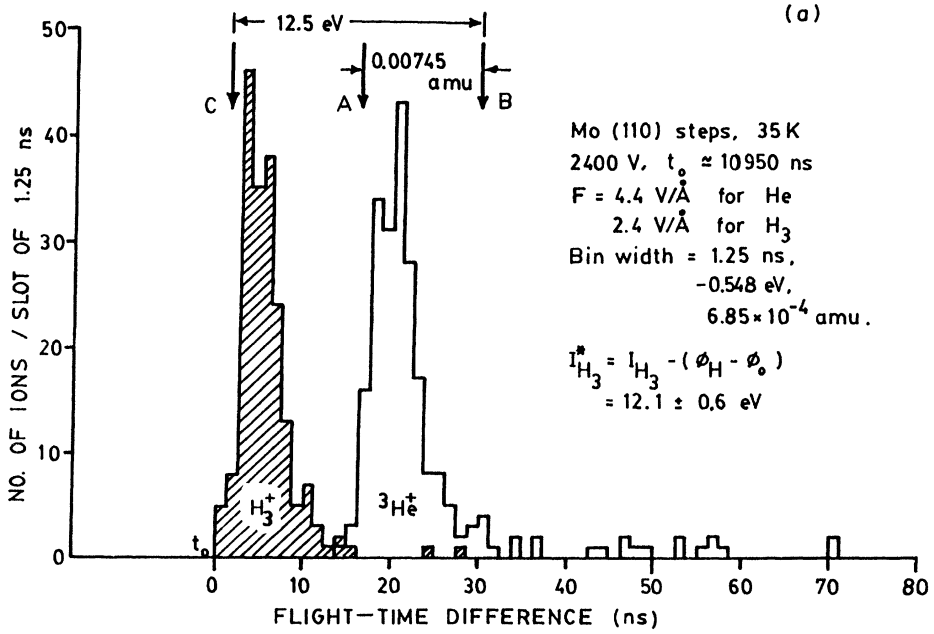

FIG. 12. (a) Energy distributions of pulsed-laser field-desorbed H_3^+ and $^3He^+$ ions taken at 2400 V. At this voltage the two mass lines are separated to near the root of the mass lines. H_3^+ distribution has no low-energy tail similar to those always found in pulsed-laser field-desorbed gaseous ions.

energy of either the equilateral H_3 molecule[32] or the collinear H_3 molecule;[29] their values are, respectively, ~ 5.7 and ~ 10.2 eV. Although these expected values, derived from both theoretical considerations and gas-phase data, have not been experimentally confirmed, it is unlikely that they will deviate more than 0.5 eV from the correct values. Thus the appearance energy we measured does not seem to represent the ionization energy of H_3 as does this measurement in pulsed-laser field desorption and field ionization of stable gases.

To help answer the question of what $I^*_{H_3}$ really represents, let us examine the energy distribution of H_3^+ more closely. Similar to the energy distribution of field-evaporated metal ions, both the H_3^+ distributions shown in Figs. 12(a) and 12(b) do not exhibit any low-energy tail. In contrast, all our pulsed-laser field-desorbed gaseous ions show persistent low-energy tails. Thus in every respect the pulsed-laser field desorption of H_3^+ resembles better the field-evaporation process. The critical-energy deficit is then given by Eq. (6),

$$I^*_{H_3} = \epsilon_c(H_3) - \phi_H \approx \Lambda + I_{H_3} - Q \approx 13.2 \text{ ,} \tag{13}$$

in units of eV. If the adsorbed H_3 is the equilateral triangular molecule, then the binding energy of H_3 with the surface will be as high as 6.5 eV. Since this is highly unlikely, we assume the field-induced chemisorbed H_3 is the collinear molecule. Since the activation energy in field desorption, Q, is small compared to other terms, we can derive the binding energy of the collinear H_3 molecule with the Mo(110) steps by omitting the Q term. It is then $\sim 3.0 \pm 0.5$ eV.

A slightly different mechanism for H_3^+ formation in field ionization has been proposed by Ernst and Block.[29] In field ionization, a H_3^+ molecule is formed at the in-

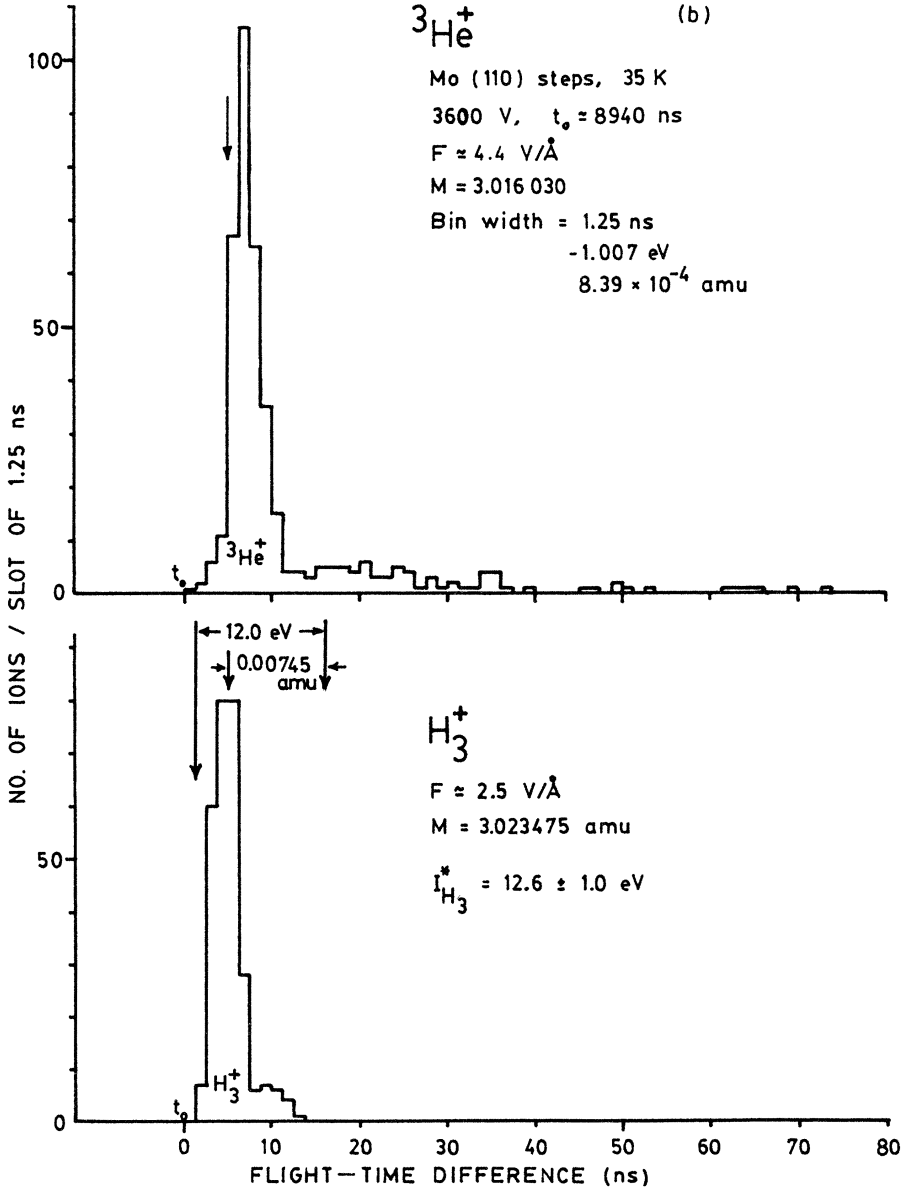

FIG. 12. (*Continued*). (b) Similar distributions taken at 3600 V. At this voltage, the two mass lines start to overlap. If the voltage is high enough, $^3He^+$ ions will eventually arrive ahead of H_3^+ ions because of the lighter mass.

stant a field-adsorbed H_2 molecule combines with a chemisorbed H molecule. In our case, this mechanism is highly improbable. When a laser pulse comes, the surface is heated up to 200—300 K for ~1 nsec. This temperature is estimated from the evaporation field of the substrate.[14] The field-adsorbed H_2 molecule will be desorbed immediately. A chemisorbed H molecule, with its > 1-eV binding energy, does not have a chance to catch up with the desorbing H_2^+. The observed H^+ results from a field dissociation of H_2^+, not from chemisorbed H.[9] We therefore favor the existence of a H_3 adsorption state in the presence of a field of 2—3 V/Å on some metal surfaces.[9] From the observed relative abundance of H_3^+ in this field range, we estimate the lifetime of H_3 to be in the millisecond range, comparable to the time needed to build up a field-adsorbed H_2 layer.

We recognize here that neither theoretical calculations nor experimental studies are complete enough to make an unequivocal determination of the mechanisms of H_3^+ formation in either pulsed-laser field desorption or in field ionization. Our suggested mechanisms are consistent with our observations and theoretical data available now. The ionization energy of H_3 may well be ~13 eV. Then H_3^+ is simply formed by field ionization of thermally desorbed H_3.

V. FORMATION OF METAL-GAS COMPLEX IONS

In the presence of a gas, metal atoms often field evaporate as metal-gas complex ions. Metal hydrides and helides are commonly seen in atom-probe field-ion microscopy. The question is where are these complex ions formed? Are they formed right at the surface or in the space near the metal surface? This latter possibility cannot be excluded if one realizes that the field at a distance of 2.5—3.0 Å from a 3 + metal ion is as high as 4.6—6.9 V/Å. The polarization binding for a He, the least polarizable atom, with the metal ion is as high as 0.15—0.32 eV,

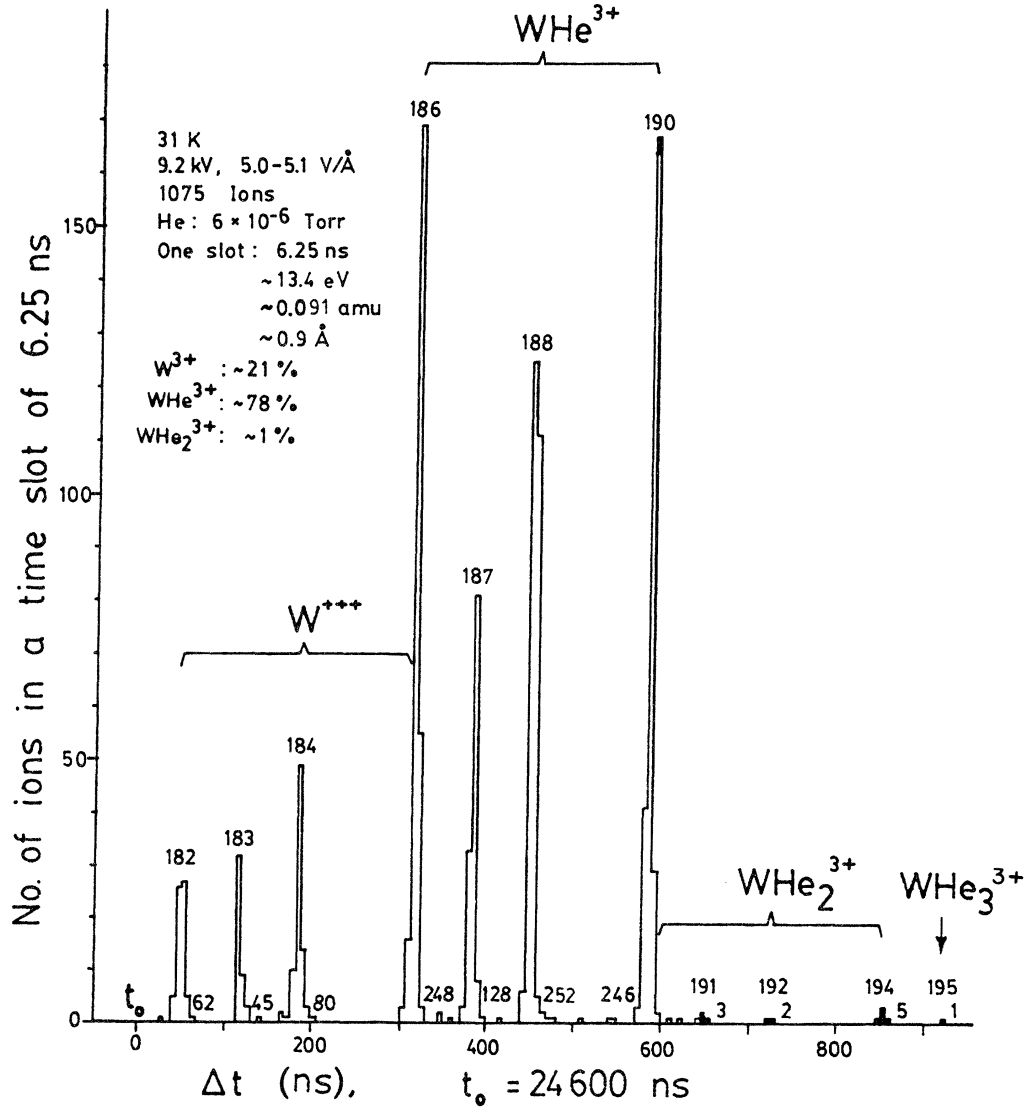

FIG. 13. Pulsed-laser field-evaporation mass spectrum of tungsten taken in the 10^{-6} Torr range of helium. Formation of tungsten monohelide and dihelide is clearly established. Energy spreads of W^{3+} and WHe^{3+} ions are comparable. No low-energy tails are seen.

enough to bind them together at low temperatures.[33] Based on a recent measurement of the ion-energy distributions in helide and hydride formation, however, we have rejected this possibility.[9] Under the conditions where $RhHe^{2+}$ and Rh^{2+} are nearly equally abundant, the energy-distribution width of $RhHe^{2+}$ is found to be much narrower than that of Rh^{2+}. Similar situations are also found in hydride formation of Au. Our conclusions in these two cases are that the complex ions are formed right at the surface whereas the metal ions detected are mostly the field-dissociated products of the complex ions. Two questions arise. (1) Does field dissociation of complex ions necessarily occur under the conditions where the complex ions can be formed? (2) Do the metal ions exhibit the same energy distribution as the complex ions when they are not formed by field dissociation of the complex ions?

These questions are answered in the tungsten and nickel data shown in Figs. 13 and 14. We find that tungsten can be pulsed-laser field-evaporated in 10^{-6} Torr of He to form more than 90% of helide ions. Helide ions are more abundant if the field evaporation is done at a low tip temperature and a high dc field. The majority of the helides are monohelide ions. About 1% of them are dihelide ions. A few trihelide and quadrahelide ions are also found but their existence cannot be assured because their masses coincide with those of WC^{3+} and WO^{3+}. The energy distributions of W^{3+} and WHe^{3+} ions are shown in Fig. 9. These are obtained by combining the major isotope lines according to their masses. Surprisingly, the W^{3+} and WHe^{3+} distributions are nearly identical. We conclude that in this case few WHe^{3+} ions are field dissociated during their flight to the detector. Both the W^{3+} and the WHe^{3+} ions are formed right at the surface during the pulsed-laser-assisted field evaporation. Although field dissociation can occur for some complex ions, some are very stable once they are formed.

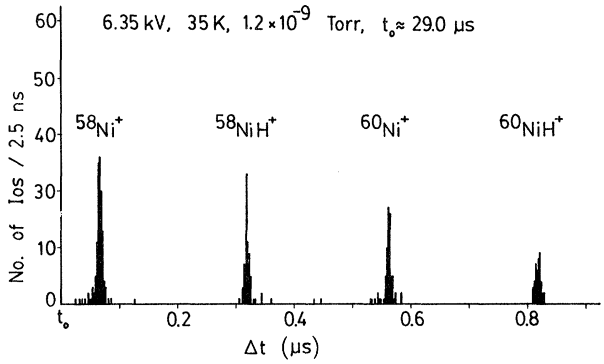

FIG. 14. Pulsed-laser field-evaporation mass spectrum of nickel taken in 8×10^{-10} to 1.5×10^{-9}-Torr vacuum. Partial pressure of hydrogen must be in the 10^{-10}-Torr range. Even under such vacuum conditions, a large fraction of nickel atoms field-evaporates as monohydride ions. Energy spreads of Ni^+ and NiH^+ ions are also comparable.

This is also true for NiH^+ ions. Once they are formed they are very stable. Thus the energy spread of Ni^+ is comparable to that of NiH^+. At the present time we have no explanation of why WHe^{3+} and NiH^+ are stable while $RhHe^{2+}$ and $AuH_2{}^+$ are unstable in a high electric field. The stability of complex, heavy ions has been a subject of great interest since it is related to relativistic corrections to Hartree-Fock calculations.[34] A systematic experimental study should shed some light on the relativistic effect in heavy atoms and ions.

ACKNOWLEDGMENTS

This work was supported by the National Science Foundation under Grant No. NSF-DMR-82-17119.

[1]R. Gomer, *Field Emission and Field Ionization* (Harvard University Press, Cambridge, Mass., 1961).
[2]E. W. Müller and T. T. Tsong, *Field Ion Microscopy, Princples and Applications* (Elsevier, New York, 1969).
[3]R. L. Seliger, J. W. Ward, V. Wang, and R. L. Kubena, Appl. Phys. Lett. 34, 310 (1979).
[4]M. G. Inghram and R. Gomer, J. Chem. Phys. 22, 1279 (1954); Z. Naturfosch. Teil A 10, 863 (1955).
[5]T. T. Tsong and E. W. Müller, J. Chem. Phys. 41, 3279 (1964).
[6]E. W. Müller and T. T. Tsong, Prog. Surf. Sci. 4, 1 (1973).
[7]S. V. Krishnaswamy and E. W. Müller, Rev. Sci. Instrum. 45, 1049 (1974).
[8]N. Ernst and Th. Jentsch, Phys. Rev. B 24, 6234 (1981).
[9](a) T. T. Tsong, T. J. Kinkus, and C. F. Ai, J. Chem. Phys. 78, 4763 (1983); (b) T. T. Tsong, T. J. Kinkus, and S. B. McLane, *ibid.* 78, 7497 (1983).
[10]T. T. Tsong, S. B. McLane, and T. J. Kinkus, Rev. Sci. Instrum. 53, 1442 (1982).
[11]H. F. Liu and T. T. Tsong (unpublished).
[12]E. W. Müller and K. Bahadur, Phys. Rev. 102, 624 (1956).
[13]A. J. Jason, R. P. Burns, A. C. Parr, and M. G. Inghram, J. Chem. Phys. 44, 4351 (1966); A. J. Jason, Phys. Rev. 156, 266 (1967).
[14]G. L. Kellogg and T. T. Tsong, J. Appl. Phys. 51, 1184 (1980).
[15]T. T. Tsong, W. A. Schmidt, and O. Frank, Surf. Sci. 65, 109 (1977).
[16]R. Gomer and L. W. Swanson, J. Chem. Phys. 39, 1913 (1963).
[17]A. A. Lucas, Phys. Rev. Lett. 26, 813 (1971).
[18]A. A. Lucas and M. Sûnjic, J. Vac. Sci. Technol. 9, 725 (1972).
[19]D. G. Brandon, Surf. Sci. 3, 1 (1964).
[20]T. T. Tsong, Surf. Sci. 10, 102 (1968).
[21]T. T. Tsong, Surf. Sci. 70, 211 (1978).
[22]E. W. Müller and S. V. Krishnaswamy, Phys. Rev. Lett. 37, 1011 (1976).
[23]R. Haydock and D. R. Kingham, Phys. Rev. Lett. 44, 1520 (1980); D. R. Kingham, Surf. Sci. 116, 273 (1982).
[24]R. S. Chambers, M. Vesely, and G. Ehrlich, in Abstracts of the 17th Field Emission Symposium, New Haven, 1970 (unpublished).

[25]N. Ernst, Surf. Sci. 87, 469 (1979).
[26]G. L. Kellogg, Surf. Sci. 120, 319 (1982).
[27]M. Konishi, M. Wada, and O. Nishikawa, Surf. Sci. 107, 63 (1981).
[28]A. J. Jason, B. Halpern, M. G. Inghram, and R. Gomer, J. Chem. Phys. 52, 2227 (1970).
[29]N. Ernst and J. H. Block, Surf. Sci. 126, 357 (1983).
[30]N. Ernst and J. H. Block, in *Proceedings of the Thirtieth International Field Emission Symposium, Philadelphia, 1983* (unpublished).
[31]R. S. Polizzotti and G. Ehrlich, J. Chem. Phys. 71, 259 (1979).
[32]R. L. Martin, J. Chem. Phys. 71, 3541 (1979).
[33]Some numerical errors are present in our original paper, pp. 4772 and 4773 of Ref. 9(a).
[34]P. Pyykkö, J. Chem. Soc. Faraday Trans. II, 75, 1256 (1978).

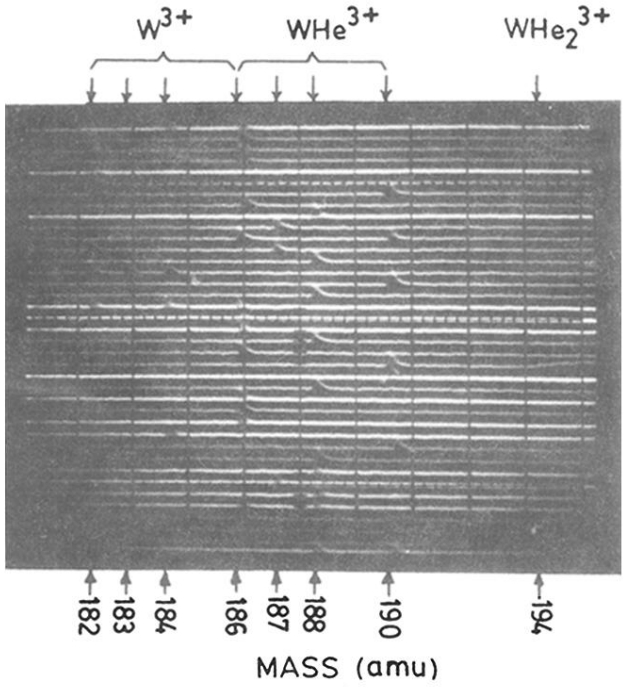

FIG. 2. Oscilloscope with 38 traces, at 0.1-μs/div speed, showing the time-of-flight signals in a study of tungsten-helide formation. Ions are detected one by one. Because of the exceptional mass resolution of this atom probe, no ambiguity exists in properly identifying the ion species even if some of them are rare.